



# THE UNIVERSITY *of* EDINBURGH

## Edinburgh Research Explorer

### **Erosion-deposition patterns and depo-center movements in branching channels at the near-estuary reach of the Yangtze River**

**Citation for published version:**

Zhu, B, Deng, J, Tang, J, Yu, W, Borthwick, AGL, Chai, Y, Sun, Z & Li, Y 2020, 'Erosion-deposition patterns and depo-center movements in branching channels at the near-estuary reach of the Yangtze River', *Frontiers in Earth Science*. <https://doi.org/10.1007/s11707-019-0808-2>

**Digital Object Identifier (DOI):**

[10.1007/s11707-019-0808-2](https://doi.org/10.1007/s11707-019-0808-2)

**Link:**

[Link to publication record in Edinburgh Research Explorer](#)

**Document Version:**

Peer reviewed version

**Published In:**

Frontiers in Earth Science

**General rights**

Copyright for the publications made accessible via the Edinburgh Research Explorer is retained by the author(s) and / or other copyright owners and it is a condition of accessing these publications that users recognise and abide by the legal requirements associated with these rights.

**Take down policy**

The University of Edinburgh has made every reasonable effort to ensure that Edinburgh Research Explorer content complies with UK legislation. If you believe that the public display of this file breaches copyright please contact [openaccess@ed.ac.uk](mailto:openaccess@ed.ac.uk) providing details, and we will remove access to the work immediately and investigate your claim.



1 **Erosion-deposition patterns and depo-center movements in**  
2 **branching channels at the near-estuary reach of the Yangtze**  
3 **River**

4  
5 **Boyuan ZHU (✉)<sup>1</sup>, Jinyun DENG<sup>2</sup>, Jinwu TANG<sup>3</sup>, Wenjun YU<sup>4</sup>,**  
6 **Alistair G.L. BORTHWICK<sup>5</sup>, Yuanfang CHAI<sup>6</sup>, Zhaohua SUN<sup>2</sup>,**  
7 **Yitian LI<sup>2</sup>**

8  
9 1 School of Hydraulic Engineering, Key Laboratory of Water-Sediment Sciences and Water  
10 Disaster Prevention of Hunan Province, Changsha University of Science & Technology, Changsha  
11 410114, China

12 2 State Key Laboratory of Water Resources and Hydropower Engineering Science, Wuhan  
13 University, Wuhan 430072, China

14 3 Changjiang Institute of Survey, Planning, Design and Research, Wuhan 430010, China

15 4 Changjiang Waterway Institute of Planning, Design & Research, Wuhan 430040, China

16 5 School of Engineering, The University of Edinburgh, The King's Buildings, Edinburgh EH9  
17 3JL, UK

18 6 Department of Earth Sciences, Vrije Universiteit Amsterdam, Boelelaan 1085, 1081 HV  
19 Amsterdam, The Netherlands

20  
21 **E-mail: boyuan@csust.edu.cn**

22 **Abstract**

23 Channel evolution and depo-center migrations in braided reaches are significantly  
24 influenced by variations in runoff. This study examines the effect of runoff variations  
25 on the erosion-deposition patterns and depo-center movements within branching  
26 channels of the near-estuary reach of the Yangtze River. We assume that variations in  
27 annual mean duration days of runoff discharges, ebb partition ratios in branching  
28 channels, and the erosional/depositional rates of entire channels and sub-reaches are  
29 representative of variations in runoff intensity, flow dynamics in branching channels,  
30 and morphological features in the channels. Our results show that the north region of  
31 Fujiangsha Waterway, the Liuhaisha branch of Rugaosha Waterway, the west branch of  
32 Tongzhousha Waterway, and the west branch of Langshansha Waterway experience  
33 deposition or reduced erosion under low runoff intensity, and erosion or reduced  
34 deposition under high runoff intensity, with the depo-centers moving upstream and  
35 downstream, respectively. Other waterway branches undergo opposite trends in  
36 erosion-deposition patterns and depo-center movements as the runoff changes. These  
37 morphological changes may be associated with trends in ebb partition ratio as the runoff  
38 discharge rises and falls. By flattening the intra-annual distribution of runoff discharge,  
39 dam construction in the Yangtze Basin has altered the ebb partition ratios in waterway  
40 branches, affecting their erosion-deposition patterns and depo-center movements.  
41 Present trends are likely to continue into the future as a succession of large cascade  
42 dams is under construction along the upper Yangtze.

43 **Keywords** near-estuary reach, Yangtze River, runoff discharge, ebb partition ratio,

44 erosion-deposition pattern, depo-center movement

## 45 **1 Introduction**

46 Morphological evolution of river systems is important to river management and  
47 regulation, and has become a growing issue over the past decades (Li et al., 2014; Zhu  
48 et al., 2017; Schletterer et al., 2019). Braided reaches are commonplace in rivers, with  
49 alternate development and shrinkage occurring between the main stem and secondary  
50 branches; such reaches often extend from the head source to the estuary (Jain and Sinha,  
51 2004; Latrubesse, 2008; Jansen and Nanson, 2010; Chen et al., 2016; Li et al., 2016;  
52 Han et al., 2018; Zhu et al., 2017, 2019). It has been established that differences in  
53 evolutionary processes between bifurcated branches are primarily caused by changes in  
54 lateral flow dynamics, driven by variations in flow discharge (i.e. upstream runoff  
55 discharge or downstream tidal discharge) (Chen et al., 2016; Han et al., 2018; Zhu et  
56 al., 2017, 2019), local human activities (e.g. channel improvement works, and sand  
57 excavation) (Kuang et al., 2014; Zheng et al., 2018; Dai and Ding, 2019), and Coriolis-  
58 induced circulation in estuarine areas (Wang et al., 2013; Li et al., 2011, 2014). Dams  
59 modulate runoff discharge in rivers worldwide and can drive the morphological  
60 evolution of braided reaches, as demonstrated by many inland rivers (Petts and Gurnell,  
61 2005; Graf, 2006; Han et al., 2018; Alcayaga et al., 2019; Mendoza et al., 2019; Zhu et  
62 al., 2019) and estuarine areas (Warne et al., 2002; Sloff et al., 2013; Zhu et al., 2017;  
63 Liu et al., 2018; Zhou et al., 2018), noting that tidal discharges are relatively stable at  
64 the yearly time scale (Horrevoets et al., 2004; Jiang et al., 2012a; Zhu et al., 2017). For  
65 fluvial braided reaches, shrinking or developing trends of branching channels are often

66 aggravated or interchanged after dam impoundment, caused by changes in  
67 unidirectional flow dynamics driven by the altered runoff discharge (Han et al., 2018;  
68 Zhu et al., 2019). However, the morphological evolution in branches of tidal-affected  
69 braided reaches (including bifurcated estuaries) are more intricate, mainly due to the  
70 complexity of bifurcating systems and the jacking effect of tidal currents (Zhang et al.,  
71 2015; Zhu et al., 2017, 2018). Marine dynamic factors, such as waves, longshore  
72 currents, and storm surges, further complicate morphological changes in estuarine areas  
73 (Kaliraj et al., 2014; Rangoonwala et al., 2016; Shen et al., 2019).

74 As the largest river on the Eurasian continent and the third longest in the world,  
75 the Yangtze has accommodated the construction of more than 50,000 dams since the  
76 1950s (Yang et al., 2011, 2015). Moreover, the Yangtze River hosts 49 major braided  
77 reaches in its middle and lower region (including the Yangtze Estuary); these reaches  
78 are classified into three main types: straight braided reaches; slightly bending braided  
79 reaches; and goose-head braided reaches (Yu, 2013). Under the impact of the dams, the  
80 intra-annual distribution of runoff discharge has flattened, whereas the total yearly  
81 runoff flux has hardly changed (Zhao et al., 2018; Zhu et al., 2017, 2018, 2019).  
82 Consequently, changes to the natural evolutionary trends of the branching channels have  
83 been generally identified in the braided reaches along the Yangtze River (Han et al.,  
84 2018; Zhu et al., 2017, 2019). Nevertheless, the braided near-estuary reach, which  
85 extends from the tidal current limit of the Yangtze River to the upper boundary-node of  
86 the Yangtze Estuary (Yu and Lu, 2005), has not yet been investigated comprehensively.  
87 Researchers have chiefly analyzed the evolutionary courses of thalwegs, cross-sections,

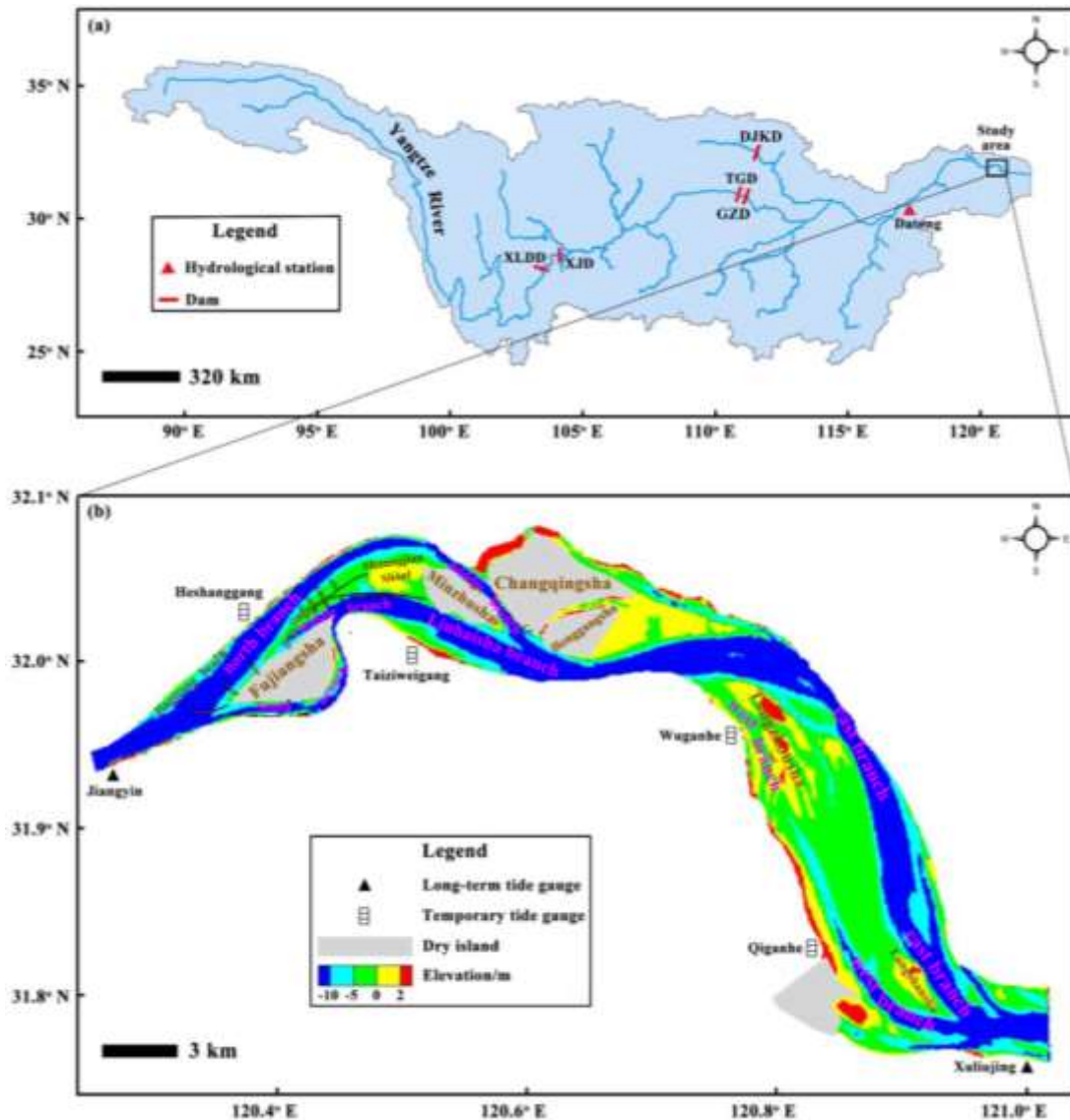
88 and flow hydrodynamics (e.g. net discharge ratios and flow velocities) in the branching  
89 channels of the near-estuary reach (Jiang et al., 2012b; Chen et al., 2012, 2016; Fan et  
90 al., 2017; Zhang and Xu, 2017), but have not considered overall variations in channel  
91 morphology and systemic relationships between erosion-deposition patterns and  
92 variations in the flow hydrodynamics. This implies that, predictions of the future  
93 evolution of branching channels in this reach (Jiang et al., 2012b; Chen et al., 2016)  
94 might be unreliable. Moreover, the law of depo-center movement in the branching  
95 channels of the near-estuary reach has not been explored. (The depo-center is defined  
96 as the location where the sediment deposition rate is a maximum.) Depo-center  
97 movement has not been considered previously for other braided reaches or river  
98 systems as well, and deserves in-depth analysis given its indicative role regarding  
99 erosion-deposition distributions in the branching channels of a braided river.

100 In the present study, the overall morphological evolution and the law of depo-  
101 center migration in branching channels of the near-estuary reach of the Yangtze River  
102 are investigated, based on terrain and hydrodynamic data from 1950 to 2014. The  
103 findings may be transferable to other braided reaches worldwide, and should be useful  
104 in guiding future engineering projects that are planned for the near-estuary reach of the  
105 Yangtze River.

## 106 **2 Study area**

107 The near-estuary reach of the Yangtze River is located at the distal section of the  
108 Yangtze River (Fig. 1(a)), extending from Jiangyin (the tidal current limit) to Xuliujing  
109 (the upper boundary-node of the Yangtze Estuary) (Yu and Lu, 2005). The reach is of

110 length  $\sim 90$  km (Fig. 1(b)). Its main braided waterways comprise the Fujiangsha,  
111 Rugaosha, Tongzhousha, and Langshansha Waterways (Fig. 1(b)). The middle branch  
112 of the Rugaosha Waterway connects with the north branch of the Fujiangsha Waterway,  
113 whilst the Liuhaisha branch of the Rugaosha Waterway connects to the middle and  
114 south branches of the Fujiangsha Waterway (Fig. 1(b)). Similarly, the east and west  
115 branches of the Langshansha Waterway connect with the corresponding branches of the  
116 Tongzhousha Waterway (Fig. 1(b)). This braided reach is influenced by tides, with  
117 multi-year (1950-2014) average tidal ranges of 1.68 and 2.04 m at Jiangyin and  
118 Xuliujing (Fig. 1(b)) (Zhu et al., 2018). Due to the relative stability of tidal forcing at  
119 the yearly time scale (Horrevoets et al., 2004; Jiang et al., 2012a; Zhu et al., 2017), the  
120 mean annual tidal level at Xuliujing (the lower boundary of this reach, Fig. 1(b)) is  
121 almost constant (Zhu et al., 2018). By comparison, runoff discharge from Datong  
122 hydrological station (Fig. 1(a)), representing the most downstream reach (Zhao et al.,  
123 2018; Zhu et al., 2017, 2018, 2019), experiences significant intra-annual variability,  
124 exhibited by a reduced flood discharge occurrence frequency and increased middle-low  
125 discharge occurrence frequency (Zhu et al., 2017, 2018, 2019). However, the annual  
126 runoff discharge is almost constant (Zhao et al., 2018; Zhu et al., 2017, 2018, 2019),  
127 with a multi-year (1950-2014) average value of  $8930 \text{ m}^3/\text{s}$  (CWRC, 2016). To achieve  
128 the national goal of a Golden Waterway, extensive channel improvements have been  
129 implemented along the near-estuary reach, including an upstream extension of the  
130 Deepwater Channel Project (Chen et al., 2012; Wu et al., 2013; Yang and Lin, 2013; Ni  
131 et al., 2014; Xu et al., 2014).



132  
 133 **Fig. 1** The Yangtze Basin and its near-estuary reach. (a) Outline map of the Yangtze Basin indicating  
 134 the locations of the Xiluodu Dam (XLDD), Xiangjia Dam (XJD), Three Gorges Dam (TGD),  
 135 Gezhou Dam (GZD), Danjiangkou Dam (DJKD), Datong hydrological station, and the near-estuary  
 136 reach (the study area). The years of impoundment of the dams were 2013, 2012, 2003, 1981 and  
 137 1968, respectively. (b) Bathymetry of the branched near-estuary reach, with positions of tide gauges  
 138 superimposed.

### 139 **3 Materials and methods**

#### 140 **3.1 Data information**

141 Observed daily runoff discharge time series at Datong station from 1950 to 2014,  
 142 and hourly ebb tidal discharges in the branching channels and hourly ebb tidal levels at  
 143 temporary tide gauges in the vicinity of the waterways from 30<sup>th</sup> August to 10<sup>th</sup>



144 September 2004 and from 17<sup>th</sup> January to 12<sup>th</sup> February 2005 were obtained from the  
145 Changjiang Water Resources Commission (China). Bed-elevation point data digitized  
146 from surveyed navigational charts in 2005 and 2007 were provided by the Shanghai  
147 Estuarine & Coastal Science Research Center (China); those in 2011 and 2014 were  
148 obtained from the Changjiang Waterway Bureau (China). Channel volumes below -5 m  
149 and -10 m isobaths in the two branches of the Tongzhousha Waterway were acquired  
150 from the Changjiang Waterway Bureau (China). The following data on hydrodynamics  
151 and morphology were gathered from the open literature: (1) yearly wet-season average  
152 ebb partition ratios for branching channels in 1977, 1983, 1993, 1998, 2006, and 2011;  
153 (2) minimum widths of -8 m and -10 m isobaths in the north branch of the Fujiangsha  
154 Waterway from 2005 to 2012; (3) cross-sectional profiles at the entrance of the south  
155 branch of the Fujiangsha Waterway in 1977, 1983, 1993, 1998, 2006, and 2011; and (4)  
156 cross-sectional areas of the two branches of the Rugaosha Waterway under bankfull  
157 discharge in 1977, 1983, 1993, 1998, 2006, and 2011. Table 1 summarizes the data  
158 sources.

159 **Table 1** Data information

Type	Name	Time	Source(s)
	Daily runoff discharge series	1950-2014	Changjiang Water Resources Commission (China)
Hydrodynamics	Hourly ebb tidal discharge series in the branching channels	2004.08.30-2004.09.10, 2005.01.17-2005.02.12	Changjiang Water Resources Commission (China)
	Hourly tidal level series at temporary tide gauges in vicinity of the waterways <sup>a)</sup>	2004.08.30-2004.09.10, 2005.01.17-2005.02.12	Changjiang Water Resources Commission (China)
	Yearly wet-season	1977, 1983, 1993, 1998,	Chen et al., 2016

	average ebb partition ratios in the branching channels	2006, 2011	
	Bed-elevation point data of the whole near-estuary reach	2005, 2007, 2011, 2014	Shanghai Estuarine & Coastal Science Research Center (China) and Changjiang Waterway Bureau (China)
	Minimum widths of -8 m and -10 m isobaths in the north branch of Fujiangsha Waterway	2005-2012	Yang and Lin, 2013
Morphology	Cross-sectional profile at the entrance of the south branch of Fujiangsha Waterway	1977, 1983, 1993, 1998, 2006, 2011	Chen et al., 2012
	Cross-sectional areas of the two branches of Rugaosha Waterway under bankfull discharge	1977, 1983, 1993, 1998, 2006, 2011	Wu et al., 2013
	Channel volumes below -5 m and -10 m isobaths in both branches of Tongzhousha Waterway	1977, 1983, 1993, 1997, 1998, 2001, 2004, 2006, 2008, 2009, 2010	Changjiang Waterway Bureau (China)

160 <sup>a)</sup> The nearby temporary tide gauges are at Heshanggang, Taiziweigang, Wuganhe, and Qiganhe  
161 stations, as indicated on Fig. 1(b).

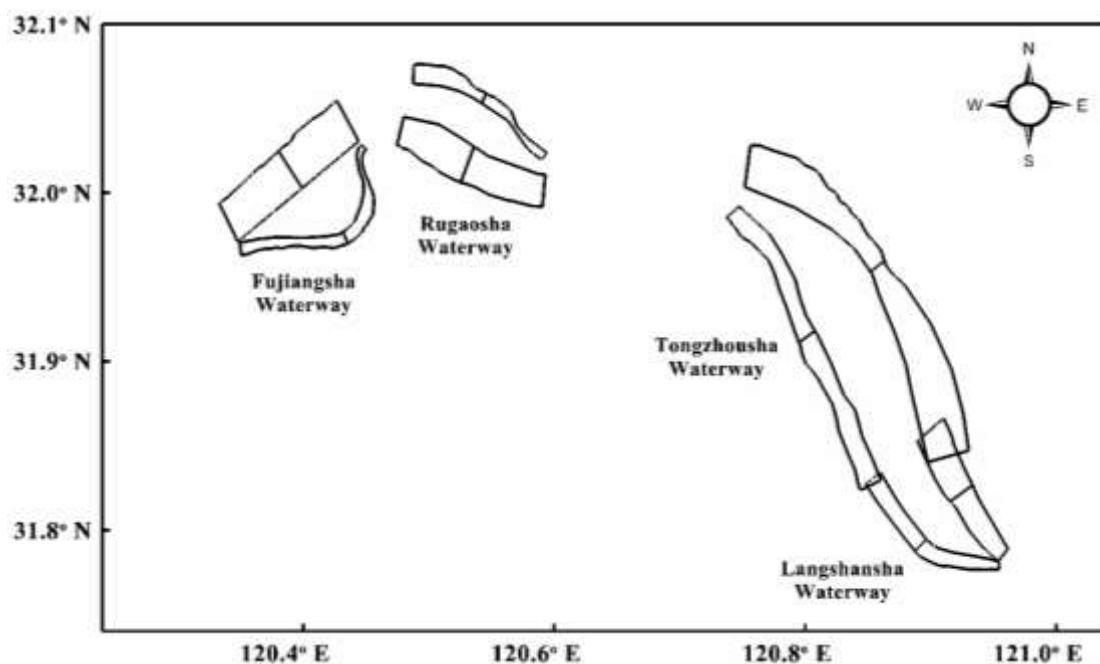
### 162 3.2 Processing of bed-elevation point data

163 Bed-elevation point data from 2005, 2007, 2011, and 2014 were projected onto  
164 Beijing 54 coordinates using ArcGIS 10.2 during digitization, with reference to 1985  
165 national elevation benchmarks. Bed elevations and point locations had previously been  
166 determined from measurements using dual-frequency echo sounders and GPS  
167 positioning. The measurement errors for bed-elevation of  $\pm 0.1$  m and location of  $\pm 1$  m  
168 were taken to be acceptable, noting the huge scale of bed-elevation changes that can  
169 occur annually (Luan et al., 2016). The proportional scales for all the four sets of terrain

170 data are 1:10,000, with sample density of 10 – 122 pts/km<sup>2</sup> (i.e. spacing of 50 – 500 m  
171 between two neighboring points), and so a grid resolution of 25 m × 250 m was adopted  
172 when calculating morphological changes using Kriging interpolation.

### 173 3.3 Interpretation of depo-centers

174 A depo-center in a branching channel is defined as the location where the  
175 maximum depositional rate of sediment occurs. Upstream and downstream depo-center  
176 movements in branching channels are identified by interpreting changes in river-bed  
177 elevation caused by erosion and deposition in upper and lower sub-reaches of roughly  
178 the same length. Increases in depositional rate or decreases in erosional rate of the upper  
179 or lower sub-reaches indicate that the depo-centers in the corresponding channels are  
180 moving towards the sub-reaches, whereas decreases in depositional rate or increases in  
181 erosional rate of the sub-reaches indicate depo-center movements away from the sub-  
182 reaches. Fig. 2 illustrates the divisions of upper and lower sub-reaches in the branching  
183 channels of the four main braided waterways.



184

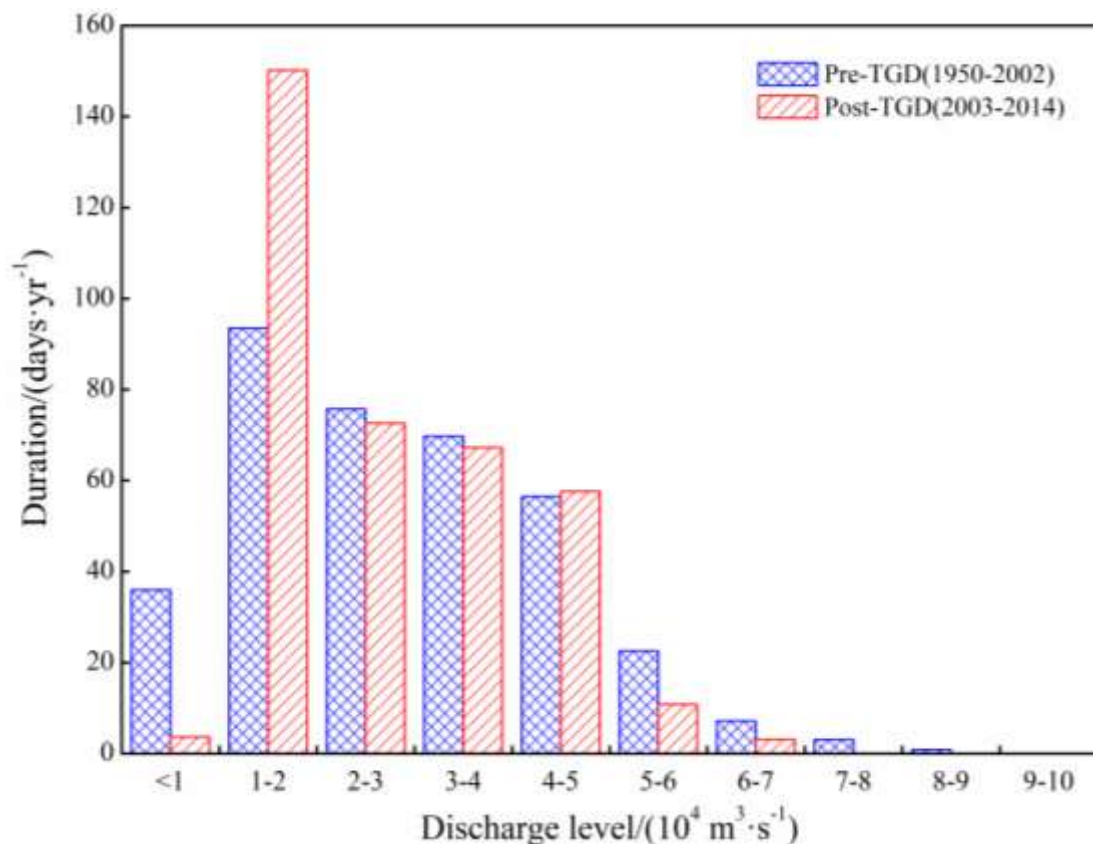
185 Fig. 2 Boundaries of branching channels and their upper and lower sub-reaches.

## 186 4 Results

### 187 4.1 Hydrodynamic variations

#### 188 4.1.1 Runoff discharge

189 Fig. 3 shows that the yearly runoff discharge changed little, whereas the intra-  
190 annual distribution of runoff discharge flattened significantly, from the pre-TGD period  
191 (in which the GZD and the DJKD impounded water, Fig. 1) before the TGD became  
192 operational to the post-TGD period (in which the TGD, the XJD and the XLDD  
193 impounded water, Fig. 1) afterwards. It can be seen that the multi-year average duration  
194 days of discharges  $< 10,000 \text{ m}^3/\text{s}$  and  $> 50,000 \text{ m}^3/\text{s}$  decreased significantly, while those  
195 of  $10,000\text{-}20,000 \text{ m}^3/\text{s}$  increased substantially.



196

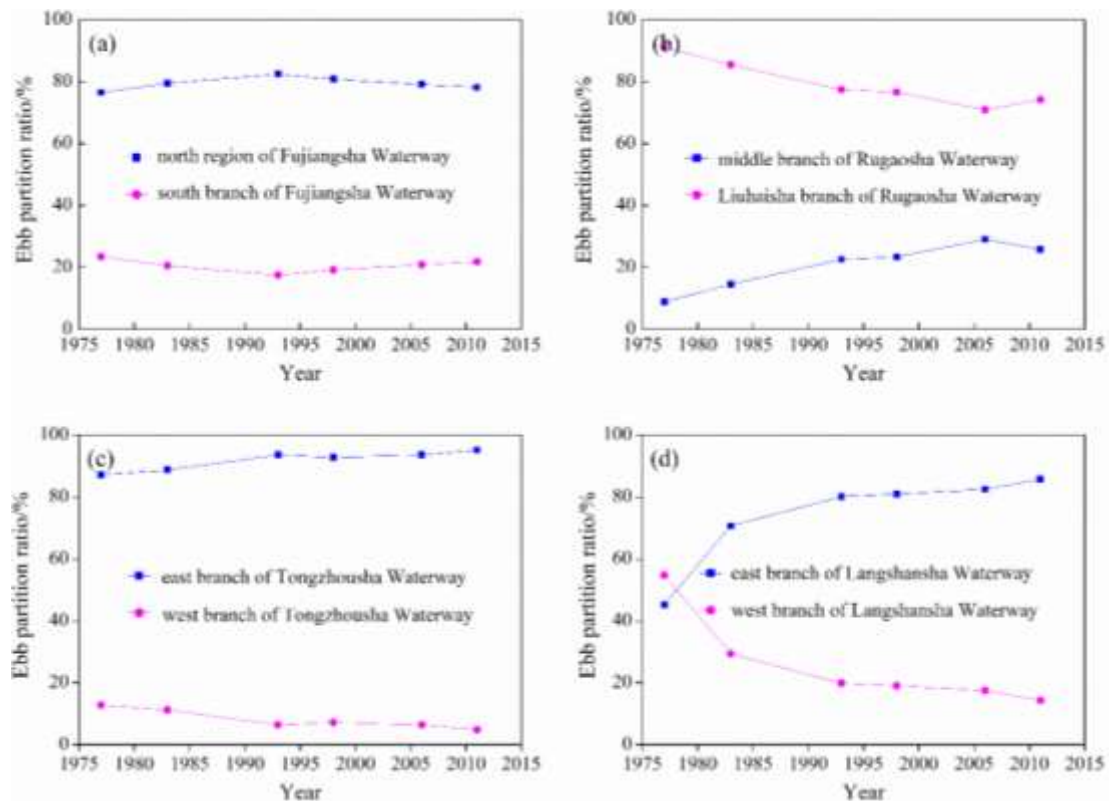
197 Fig. 3 Histogram of annual mean duration days for different runoff discharge levels at Datong station  
198 from 1950 to 2002 before impoundment of the TGD (and also XJD and XLDD, Fig. 1(a)) and from

199 2003 to 2014 after its impoundment, during which time both XLDD and XJD also commenced  
200 operation.

#### 201 4.1.2 Ebb partition ratio

##### 202 4.1.2.1 Yearly trends

203 Fig. 4 shows that the yearly wet-season average ebb partition ratios in the north  
204 region (including the north branch, middle branch, and Shuangjian shoal, Fig. 1(b)) of  
205 Fujiangsha Waterway, the Liuhaisha branch of Rugaosha Waterway, the west branch of  
206 Tongzhousha Waterway, and the west branch of Langshansha Waterway exhibited  
207 decreasing trends from 1977 to 2011, whereas the ebb partition ratios for the other  
208 branches of the four waterways presented increasing trends.

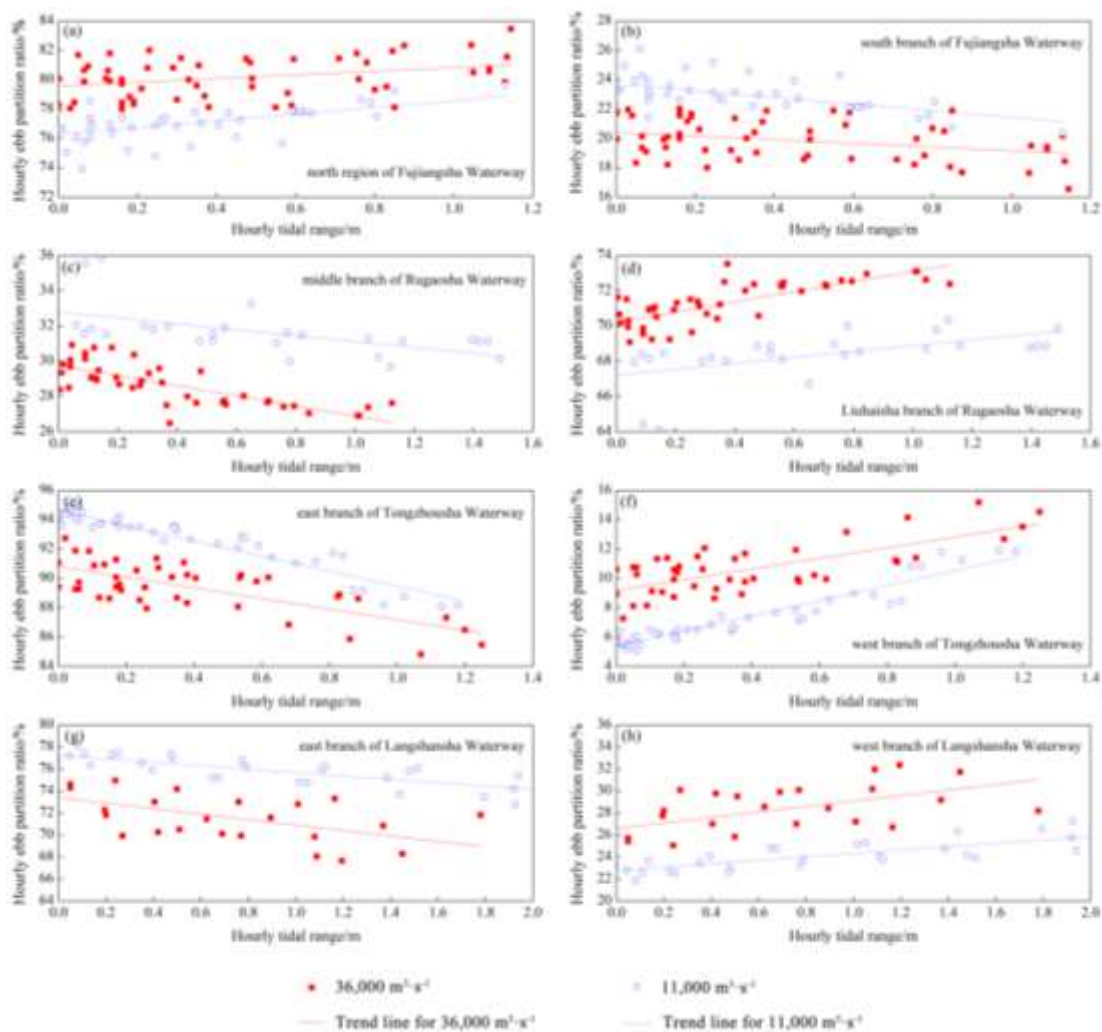


209  
210 **Fig. 4** Trends in annual wet-season average ebb partition ratios for branching channels of the  
211 following waterways: (a) Fujiangsha; (b) Rugaosha; (c) Tongzhousha; and (d) Langshansha.

##### 212 4.1.2.2 Changes under different runoff conditions

213 Fig. 5 presents the variations in ebb partition ratio with tidal range obtained for the

214 branching channels from 30<sup>th</sup> August to 10<sup>th</sup> September 2004 and from 17<sup>th</sup> January to  
 215 12<sup>th</sup> February 2005, for runoff discharges of 36,000 m<sup>3</sup>/s and 11,000 m<sup>3</sup>/s. The tidal data  
 216 were obtained using temporary tide gauges (see Fig. 1(b) for locations). For all tidal  
 217 range values considered, the ebb partition ratio at a runoff discharge of 36,000 m<sup>3</sup>/s was  
 218 invariably larger than that at 11,000 m<sup>3</sup>/s in the north region of Fujiangsha Waterway,  
 219 the Liuhaisha branch of Rugaosha Waterway, the west branch of Tongzhousha  
 220 Waterway, and the west branch of Langshansha Waterway. This implies that the higher  
 221 runoff discharge caused flow to divert into these branches, with the opposite occurring  
 222 in the other waterway branches.



223  
 224 **Fig. 5** Relationships between ebb partition ratio and tidal range for two runoff discharge levels in

225 the branching channels of the waterways: (a) north region of Fujiangsha Waterway; (b) south branch  
226 of Fujiangsha Waterway; (c) middle branch of Rugaosha Waterway; (d) Liuhaisha branch of  
227 Rugaosha Waterway; (e) east branch of Tongzhousha Waterway; (f) west branch of Tongzhousha  
228 Waterway; (g) east branch of Langshansha Waterway; and (h) west branch of Langshansha  
229 Waterway. Each hourly tidal range value was determined by subtracting the average of preceding  
230 and succeeding low tidal levels from the hourly tidal level.

## 231 4.2 Morphological variations

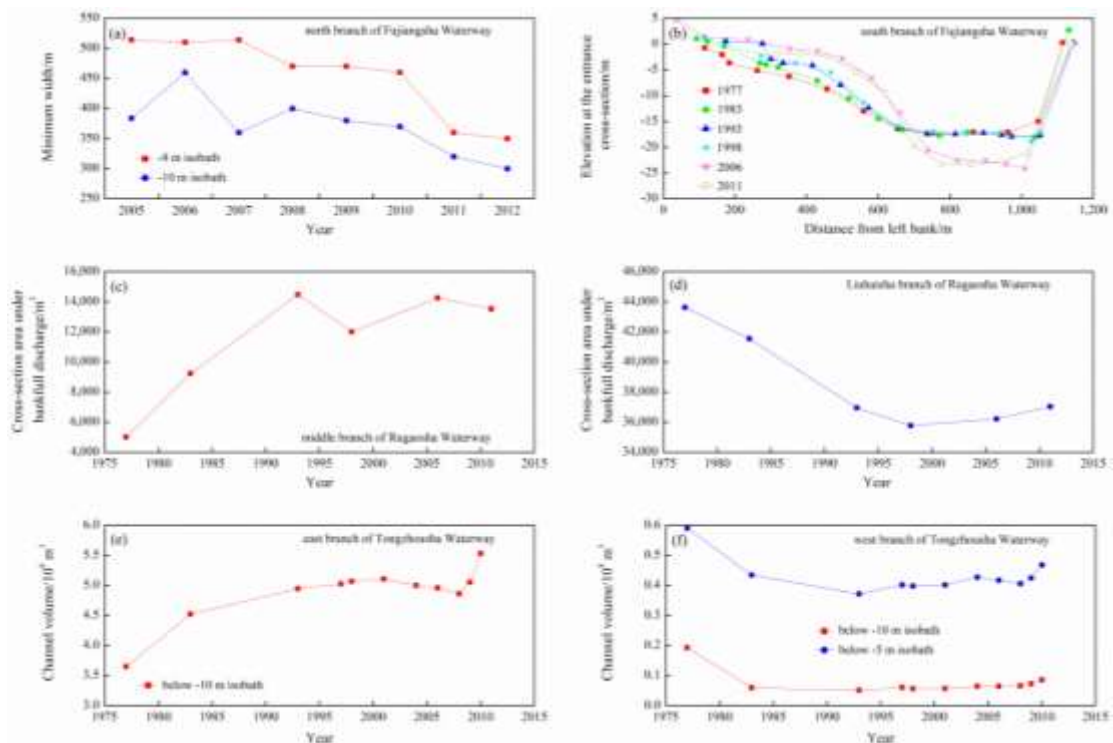
### 232 4.2.1 Whole channel

#### 233 4.2.1.1 Yearly trends

234 Both the annual time series of minimum widths of the -8 m and -10 m isobaths in  
235 the north branch of the Fujiangsha Waterway present decreasing temporal trends (Fig.  
236 6(a)), indicating that the north branch has been progressively shrinking. Given that the  
237 north branch is the main channel at the north of Fujiangsha Island (Fig. 1(b)), this  
238 shrinkage implies that the northern region (including the north branch, middle branch,  
239 and Shuangjian shoal) of the Fujiangsha Waterway has been experiencing  
240 morphological decline. By contrast, the deep channel of the cross-section at the  
241 entrance of the south branch of Fujiangsha Waterway underwent significant erosion  
242 from 1977 to 2011 (Fig. 6(b)), suggesting the morphology of the south branch was  
243 undergoing rapid development. The cross-sectional areas of the middle branch and the  
244 Liuhaisha branch of Rugaosha Waterway presented increasing and decreasing trends  
245 under bankfull discharge (Figs. 6(c-d)), implying the middle branch and Liuhaisha  
246 branch were experiencing developing and declining morphological trends respectively.  
247 Figs. 6(e-f) show that the channel volume below the -10 m isobath in the east branch of  
248 the Tongzhousha Waterway has been presenting an increasing trend, whereas that below  
249 the -5 m and -10 m isobaths in the west branch of the Tongzhousha Waterway has a

250 decreasing trend, indicating development and decline of the east and west branches  
 251 respectively.

252 It should be noted that field observations by Chen et al. (2016) have shown that  
 253 the east and west branches of the Langshansha Waterway have exhibited developing  
 254 and declining trends.



255  
 256 **Fig. 6** Evolution of the branching channels of the waterways: (a) annual values of minimum widths  
 257 of -8 m and -10 m isobaths in the north branch of Fujiangsha Waterway; (b) evolution of the cross-  
 258 section at the entrance of the south branch of Fujiangsha Waterway; (c) annual time series of the  
 259 cross-sectional area under bankfull discharge of the middle branch of Rugaosha Waterway; (d)  
 260 evolution of the cross-sectional area under bankfull discharge of Liuhaisha branch of Rugaosha  
 261 Waterway; (e) temporal behavior of channel volume below -10 m isobath of the east branch of  
 262 Tongzhousha Waterway; and (f) temporal behavior of channel volume below -10 m and -5 m  
 263 isobaths of the west branch of Tongzhousha Waterway.

264 4.2.1.2 Changes under different runoff conditions

265 Table 2 lists erosion-deposition rates in the branching channels and the  
 266 corresponding duration days of relevant runoff discharges during 2005-2007, 2007-  
 267 2011, and 2011-2014. Fig. 7 displays plan distributions of erosion-deposition rates for



268 the whole near-estuary reach in 2005, 2007, 2011, and 2014. Of these periods, 2005-  
269 2007 was the driest, being associated with the least duration days of flood discharges (>  
270 50,000 m<sup>3</sup>/s and > 60,000 m<sup>3</sup>/s) and the most duration days of low and middle-low  
271 discharges (< 10,000 m<sup>3</sup>/s and 10,000 - 20,000 m<sup>3</sup>/s) (Table 2). This is because the  
272 2005-2007 period contained an extreme dry year event that affected the Yangtze Basin  
273 in 2006 (Zhu et al., 2018); during this event no discharge exceeded 40,000 m<sup>3</sup>/s, and  
274 the duration days of low and middle-low discharges were at 7 days and 185 days. The  
275 2007-2011 period was wettest, with the largest number of duration days for flood  
276 discharges (especially > 60,000 m<sup>3</sup>/s) and lower numbers of duration days for low and  
277 middle-low discharges than in 2005-2007 (Table 2). The 2007-2011 period included the  
278 flood year of 2010 (Zhu et al., 2018), the only year during which the discharge exceeded  
279 60,000 m<sup>3</sup>/s in the total period from 2005 to 2014. In 2010, the duration of the > 60,000  
280 m<sup>3</sup>/s discharge lasted 36 days. The runoff intensity in 2011-2014 was between that in  
281 the foregoing two periods (Table 2).

282 The entire northern region of Fijiangsha Waterway (including the north branch,  
283 middle branch, and Shuangjian shoal) experienced deposition during 2005-2007, severe  
284 erosion during 2007-2011, and slight erosion during 2011-2014 (Table 2), indicating  
285 that low and high values of runoff intensity promoted deposition and erosion  
286 respectively. This erosion-deposition behavior in the north region is also confirmed by  
287 changes in the deep channel area (see Fig. 7), which shrank in the period from 2005 to  
288 2007 (Figs. 7(a-b)) before experiencing significant growth from 2007 to 2011 (Figs.  
289 7(b-c)) and from 2011 to 2014 (Figs. 7(c-d)). Erosion occurred in the south branch

290 during all three periods, with a much larger erosional rate during 2005-2007 than 2011-  
291 2014 (Table 2). Even though severe erosion occurred in the south branch during 2007-  
292 2011 when the largest number of flood discharge duration days were experienced, the  
293 rate of erosion was smaller than in the north region (Table 2; Figs. 7(b-c)). This implies  
294 that the north region and south branch underwent roughly the reverse erosion-  
295 deposition behavior under runoff changes.

296 In accordance with changes in runoff intensity, the Liuhaisha branch of Rugaosha  
297 Waterway experienced deposition during 2005-2007, significant erosion during 2007-  
298 2011, and less significant erosion during 2011-2014 (Table 2). This erosion-deposition  
299 behavior was linked to changes in the deep channel area (Fig. 7) which witnessed  
300 obvious shrinkage from 2005 to 2007 (Figs. 7(a-b)) and significant growth from 2007  
301 to 2011 (Figs. 7(b-c)) and 2011 to 2014 (Figs. 7(c-d)). The middle branch of Rugaosha  
302 Waterway exhibited a similar erosion-deposition pattern to that of the Liuhaisha branch  
303 (Table 2), influenced by the flood-tide-driven sediment supply from the lower two  
304 braided waterways during the dry period of 2005-2007 (Zhu et al., 2018) and  
305 engineering projects implemented in the vicinity (Fig. 1(b); Chen et al., 2012; Wu et al.,  
306 2013).

307 The two branches of Tongzhousha Waterway did not exhibit opposite erosion-  
308 deposition patterns under runoff change (Table 2); this was perhaps because the gradual  
309 decline of the west branch in recent years (Ni et al., 2014) caused the Tongzhousha  
310 Waterway effectively to become a single river channel dominated by the east branch.  
311 In this case, the discharge, regardless of runoff intensity, passed mainly through the east

312 branch, leading to erosion or deposition depending on the flow speed within the branch  
313 (Table 2). Meanwhile, regulation projects implemented along the Tongzhousha  
314 Waterway also impacted on the erosion-deposition pattern (Ni et al., 2014). Even so,  
315 the low runoff intensity during 2005-2007 promoted shrinkage of the west branch and  
316 shortened the deep channel of the west branch (Figs. 7(a-b)), whereas the high runoff  
317 intensities during 2007-2011 and 2011-2014 facilitated development of the west branch,  
318 lengthening its deep channel (Figs. 7(b-c) and 7(c-d)). The upper and lower deep  
319 channels became connected within the west branch from 2011 to 2014 (Figs. 7(c-d)).

320 Depositional rates in the east branch of Langshansha Waterway were smallest  
321 during 2005-2007 and largest during 2007-2011 (Table 2), indicating that low and high  
322 runoff intensities respectively facilitated the development and decline of the east branch.  
323 As shown in Fig. 7, the deep channel area in the east branch experienced obvious  
324 growth from 2005 to 2007, and altered from a bifurcating to a single channel pattern as  
325 its width increased (Figs. 7(a-b)). However, from 2007 to 2011 and 2011 to 2014 the  
326 deep channel area re-established a bifurcated pattern, with decreased width (Figs. 7(b-  
327 c) and 7(c-d)). The west branch underwent an almost opposite erosion-deposition  
328 pattern, with deposition during 2005-2007 and 2011-2014, and erosion during 2007-  
329 2011 (Table 2); this implied that low runoff intensity promoted shrinkage of the west  
330 branch whereas high runoff intensity promoted growth. Meanwhile, the deep channel  
331 of the west branch shortened during 2005-2007 (Figs. 7(a-b)) and lengthened during  
332 2007-2011 (Figs. 7(b-c)) and 2011-2014 (Figs. 7(c-d)).

333 In summary, low runoff intensity generally promoted development of the south

334 branch of Fujiangsha Waterway, the middle branch of Rugaosha Waterway, the east  
335 branch of Tongzhousha Waterway, and the east branch of Langshansha Waterway, while  
336 usually facilitating morphodynamic decline of the other branches of the braided  
337 waterways. High runoff intensity produced essentially the opposite effect.

338 **Table 2** Erosional/depositional rates (deposition positive-valued, and erosion negative-valued) of branching channels at the near-estuary reach of the Yangtze River  
 339 over different periods, and corresponding multi-year average duration days of different runoff discharges at Datong station

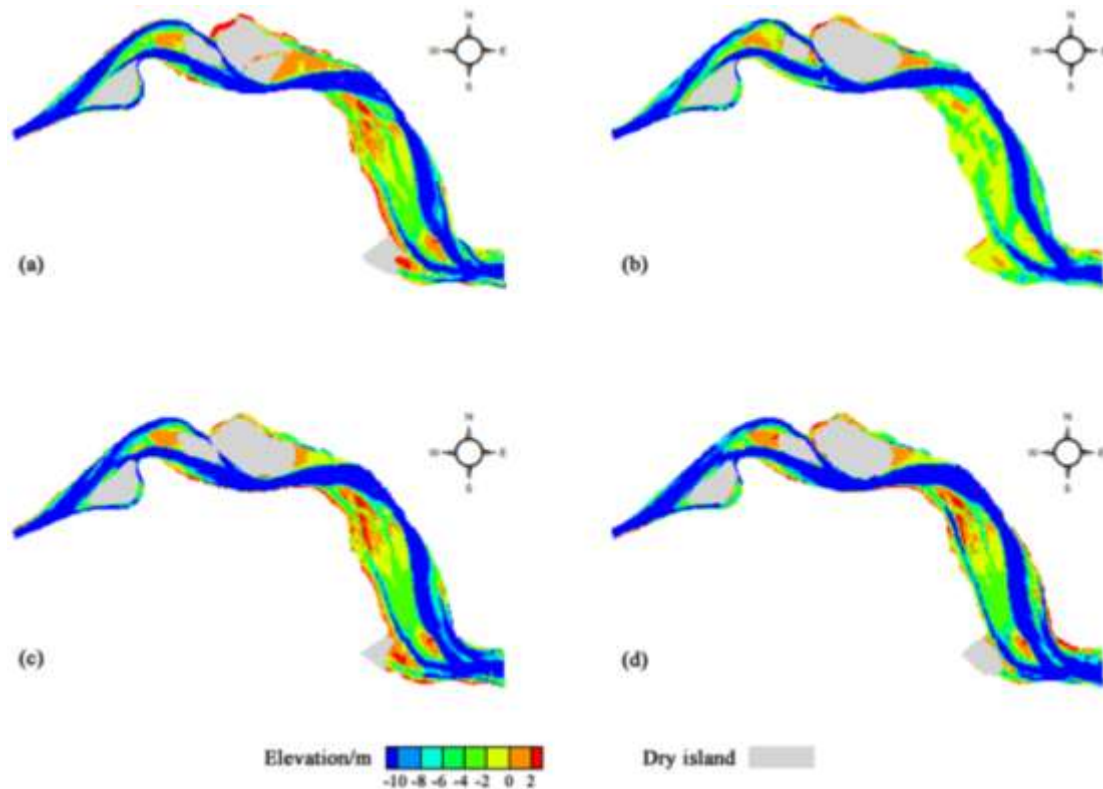
Waterway	Branching channel	Period	Erosional/Depositional rate/(m·yr <sup>-1</sup> ) <sup>a)</sup>	Annual mean duration days of runoff discharge at Datong station/(days·yr <sup>-1</sup> ) <sup>b)</sup>			
				<10,000 m <sup>3</sup> ·s <sup>-1</sup>	10,000-20,000 m <sup>3</sup> ·s <sup>-1</sup>	>50,000 m <sup>3</sup> ·s <sup>-1</sup>	>60,000 m <sup>3</sup> ·s <sup>-1</sup>
Fujiangsha	north region	2005-2007	0.650	4	170	10	0
		2007-2011	-0.458	0	168	14	7
		2011-2014	-0.186	0	156	14	0
	south branch	2005-2007	-0.147	4	170	10	0
		2007-2011	-0.314	0	168	14	7
		2011-2014	-0.020	0	156	14	0
Rugaosha	middle branch	2005-2007	0.348	4	170	10	0
		2007-2011	-0.603	0	168	14	7
		2011-2014	-0.123	0	156	14	0
	Liuhaisha branch	2005-2007	0.902	4	170	10	0
		2007-2011	-0.224	0	168	14	7
		2011-2014	-0.156	0	156	14	0
Tongzhousha	east branch	2005-2007	0.310	4	170	10	0

		2007-2011	-0.147	0	168	14	7
		2011-2014	0.024	0	156	14	0
		2005-2007	-0.095	4	170	10	0
	west branch	2007-2011	-0.018	0	168	14	7
		2011-2014	-0.678	0	156	14	0
		2005-2007	0.005	4	170	10	0
	east branch	2007-2011	0.711	0	168	14	7
		2011-2014	0.201	0	156	14	0
Langshansha		2005-2007	0.458	4	170	10	0
	west branch	2007-2011	-0.229	0	168	14	7
		2011-2014	0.767	0	156	14	0

340 a) Fig. 2 shows boundaries of the branching channels.

341 b) < 10,000 m<sup>3</sup>/s, 10,000-20,000 m<sup>3</sup>/s and > 50,000 m<sup>3</sup>/s are the discharge levels experiencing obvious changes in duration days over different periods (Fig. 3), whereas

342 60,000 m<sup>3</sup>/s approximates the bed-forming discharge in the near-estuary reach of the Yangtze River (Yun, 2004).



343

344 **Fig.7** Plan distributions of river bed elevation at the near-estuary reach of the Yangtze River in (a)  
 345 2005, (b) 2007, (c) 2011, and (d) 2014.

#### 346 4.2.2 Depo-center movement

347 The data listed in Table 3 indicate that depo-centers in the north region of  
 348 Fujiangsha Waterway, the Liuhaisha branch of Rugaosha Waterway, the west branch of  
 349 Tongzhousha Waterway, and the west branch of Langshansha Waterway moved  
 350 upstream when the runoff intensity declined, and moved downstream when runoff  
 351 intensity rose. The situation for the other branches of the waterways was quite the  
 352 opposite. The details are as follows:

353 In the north region of the Fujiangsha Waterway, the depositional rate in the upper  
 354 sub-reach was larger than in the lower sub-reach during 2005-2007 (with low runoff  
 355 intensity) (Table 3), indicating that the depo-center of this region was located in the  
 356 upper sub-reach. However, both sub-reaches experienced erosion during 2007-2011 and  
 357 2011-2014 (with higher runoff intensities) (Table 3), implying that the depo-center

358 moved into the channel downstream of this region. Moreover, because runoff intensity  
359 during 2007-2011 was higher than during 2011-2014, the erosion rates of the two sub-  
360 reaches during 2007-2011 were larger than during 2011-2014, and the erosion rate in  
361 the upper sub-reach was larger than in the lower sub-reach during 2007-2011 (Table 3).  
362 This suggested that the depo-center moved further downstream during 2007-2011 than  
363 2011-2014. Due to the likely impacts of regulation projects in the Fujiangsha Waterway  
364 (Fig. 1(b); Xu et al., 2014), the depo-center in the south branch did not exhibit the  
365 reverse behavior (Table 3).

366 The depositional rate in the lower sub-reach of the middle branch of Rugaosha  
367 Waterway was larger than in its upper sub-reach during 2005-2007 (Table 3), indicating  
368 that the depo-center was located in the lower sub-reach. During 2007-2011, both sub-  
369 reaches underwent erosion (Table 3), implying that the depo-center was located in the  
370 channel downstream of the middle branch. However, the erosional rate in the upper  
371 sub-reach was smaller than in the lower sub-reach during 2007-2011 (Table 3). This  
372 suggests that the downstream movement of the depo-center was eased by an upstream  
373 transport of sediment (eroded from the lower sub-reach during flood-tide) into the upper  
374 sub-reach during this flood period. The runoff intensity from 2011 to 2014 had a value  
375 between those during 2005-2007 and 2007-2011, and so the position of the depo-center  
376 (reflected by the erosion-deposition rates of the two sub-reaches, Table 3) occupied an  
377 intermediate location. The depo-center in the Liuhaisha branch exhibited almost the  
378 opposite behavior. Both sub-reaches of the Liuhaisha branch experienced deposition  
379 during 2005-2007 and erosion during 2007-2011 and 2011-2014 (Table 3), suggesting



380 that the depo-center was located in the Liuhaisha branch during the former period but  
381 in the channel downstream of the Liuhaisha branch during the latter two periods. In  
382 short, the depo-center migrated downstream from 2005 to 2014. Meanwhile, the  
383 decrease in erosional rate of the upper sub-reach was larger than that of the lower sub-  
384 reach from 2007-2011 to 2011-2014 as runoff intensity fell (Table 3), indicating  
385 upstream migration of the depo-center.

386 Both sub-reaches of the east branch of the Tongzhousha Waterway experienced  
387 erosion during 2007-2011 (Table 3), corresponding to the depo-center being located in  
388 the channel downstream of the east branch. However, the erosional rate in the upper  
389 sub-reach was smaller than in the lower sub-reach (Table 3). This meant that erosion in  
390 the upper sub-reach was relieved by upstream transport of sediment (eroded from the  
391 lower sub-reach by the flood-tide) into the upper sub-reach. During 2005-2007 and  
392 2011-2014, the upper and lower sub-reaches underwent erosion and deposition (Table  
393 3), implying that the depo-center was located in the lower sub-reach. In the west branch,  
394 the upper and lower sub-reaches respectively experienced erosion and deposition  
395 during 2005-2007 (Table 3), indicating that the depo-center was located in the lower  
396 sub-reach. However, both sub-reaches experienced erosion during 2011-2014, with the  
397 erosional rate of the upper sub-reach increasing significantly (Table 3), as the depo-  
398 center moved into the channel downstream of the west branch.

399 During 2005-2007, the upper and lower sub-reaches of the east branch of the  
400 Langshansha Waterway experienced erosion and deposition, respectively (Table 3),  
401 with the depo-center accordingly located in the lower sub-reach. During 2007-2011 and

402 2011-2014, the upper sub-reach accreted sediment, whilst the lower sub-reach  
403 underwent deposition (during 2007-2011) followed by erosion (during 2011-2014)  
404 (Table 3), meaning that the depo-center moved upstream, even entering the upper sub-  
405 reach. The upper and lower sub-reaches of the west branch experienced deposition and  
406 erosion respectively during 2005-2007 and 2011-2014 (Table 3) when the depo-center  
407 was located in the upper sub-reach. However, the upper and lower sub-reach underwent  
408 erosion and deposition respectively during 2007-2011 (Table 3), as the depo-center  
409 migrated downstream in the lower sub-reach during this flood period.

410 **Table 3** Erosional/depositional rates (deposition positive-valued, and erosion negative-valued) for upper and lower sub-reaches of the branching channels at the near-  
 411 estuary reach of the Yangtze River over different periods and corresponding multi-year average duration days of different runoff discharges at Datong station

Waterway	Branching channel	Period	Erosional/Depositional rate of upper sub-reach/(m·yr <sup>-1</sup> ) <sup>a)</sup>	Erosional/Depositional rate of lower sub-reach/(m·yr <sup>-1</sup> ) <sup>a)</sup>	Annual mean duration days of runoff discharges at Datong station/(days·yr <sup>-1</sup> ) <sup>b)</sup>			
					<10,000 m <sup>3</sup> ·s <sup>-1</sup>	10,000-20,000 m <sup>3</sup> ·s <sup>-1</sup>	>50,000 m <sup>3</sup> ·s <sup>-1</sup>	>60,000 m <sup>3</sup> ·s <sup>-1</sup>
Fujiangsha	north region	2005-2007	1.083	0.212	4	170	10	0
		2007-2011	-0.553	-0.359	0	168	14	7
		2011-2014	-0.170	-0.211	0	156	14	0
	south branch	2005-2007	0.802	-1.331	4	170	10	0
		2007-2011	-0.481	-0.087	0	168	14	7
		2011-2014	0.089	-0.131	0	156	14	0
Rugaosha	middle branch	2005-2007	0.091	0.820	4	170	10	0
		2007-2011	-0.383	-1.023	0	168	14	7
		2011-2014	-0.543	0.635	0	156	14	0
	Liuhaisha branch	2005-2007	0.487	1.437	4	170	10	0
		2007-2011	-0.203	-0.308	0	168	14	7
		2011-2014	-0.038	-0.265	0	156	14	0
Tongzhousha	east branch	2005-2007	-0.229	0.708	4	170	10	0
		2007-	-0.113	-0.172	0	168	14	7

		2011-2014	-0.668	0.535	0	156	14	0
		2005-2007	-0.260	0.036	4	170	10	0
	west branch	2007-2011	0.324	-0.293	0	168	14	7
		2011-2014	-1.444	-0.063	0	156	14	0
		2005-2007	-0.579	0.778	4	170	10	0
	east branch	2007-2011	0.507	0.982	0	168	14	7
		2011-2014	0.588	-0.311	0	156	14	0
Langshansha		2005-2007	0.938	-0.122	4	170	10	0
	west branch	2007-2011	-0.433	0.017	0	168	14	7
		2011-2014	1.977	-0.681	0	156	14	0

412 a) Fig. 2 shows boundaries of upper and lower sub-reaches of the branching channels.

413 b) < 10,000 m<sup>3</sup>/s, 10,000-20,000 m<sup>3</sup>/s and > 50,000 m<sup>3</sup>/s are the discharge levels experiencing obvious changes in duration days over periods (Fig. 3), whereas 60,000  
414 m<sup>3</sup>/s approximates the bed-forming discharge in the near-estuary reach of the Yangtze River (Yun, 2004).

## 415 **5 Discussion**

### 416 5.1 Linkage-mode between channel erosion-deposition and depo-center movement

417 Through the foregoing analysis, a linkage-mode can be identified between the  
418 erosion-deposition patterns of branching channels and their depo-center movements.  
419 That is, as a channel experiences erosion/deposition, its depo-center tends to move  
420 downstream/upstream. In the north part of Fujiangsha Waterway, the Liuhaisha branch  
421 of Rugaosha Waterway, the west branch of Tongzhousha Waterway, and the west branch  
422 of Langshansha Waterway, erosion and concomitant downstream depo-center migration  
423 occur as runoff intensity increases, whereas deposition and accompanying upstream  
424 depo-center migration occur as runoff intensity falls (Table 2; Fig. 7; Table 3). In other  
425 branches of the waterways, the two cases of erosion-deposition behavior and  
426 concomitant depo-center migration occur as runoff intensity falls and rises, respectively  
427 (Table 2; Fig. 7; Table 3).

### 428 5.2 Mechanism behind the linkage-mode

429 Fig. 5 indicates that there is a robust relationship between ebb partition ratio and  
430 runoff discharge for a branching channel in the near-estuary reach, given that the  
431 morphological changes in the river bed are small, owing to the short timespan from the  
432 wet period (30<sup>th</sup> August to 10<sup>th</sup> September 2004) to the dry period (17<sup>th</sup> January to 12<sup>th</sup>  
433 February 2005), and because runoff intensity was weak during this water-recession  
434 timespan. The relationships in Fig. 5 are driven by the geographic features of the near-  
435 estuary reach. Several raised nodes (formed by mountains) exist along the south bank  
436 at the entrance of Fujiangsha Waterway (Chen et al., 1988). These nodes tend to drive

437 the ebb tidal current into the north region of Fujiangsha Waterway, with this effect  
438 strengthening as runoff intensity rises (Chen et al., 1988). Hence, a high runoff  
439 discharge corresponds to a high value of ebb partition ratio in the north region and a  
440 low value of ebb partition ratio in the south branch, with the reverse occurring for a low  
441 runoff discharge (Figs. 5(a-b)). The Liuhaisha branch of Rugaosha Waterway is much  
442 wider than the middle branch of Rugaosha Waterway and connects with the north region  
443 of Fujiangsha Waterway (Fig. 1(b)). Hence, a high runoff discharge also facilitates  
444 diversion of the ebb tidal current into the Liuhaisha branch while restraining diversion  
445 of the ebb tidal current into the middle branch (Figs. 5(c-d); Chen et al., 2012). Given  
446 that the cross-section and water depth of the east branch of Tongzhousha Waterway are  
447 much larger than those of the west branch (Fig. 1(b)), the ebb tidal current tends to flow  
448 into the east branch when the runoff discharge is low, which increases the ebb partition  
449 ratio in the east branch and decreases the ebb partition ratio in the west branch (Figs.  
450 5(e-f)). Conversely, the tidal level rises as runoff discharge increases, causing part of  
451 the ebb tidal current to divert into the west branch (Chen et al., 2012), leading to the  
452 ebb partition ratio exhibiting opposite behavior in the two branches (Figs. 5(e-f)). Given  
453 that the two branches of Langshansha Waterway connect directly with those of  
454 Tongzhousha Waterway (Fig. 1(b)), the relationships between ebb partition ratio and  
455 runoff discharge of the branches are similar to those for the Tongzhousha Waterway  
456 (Figs. 5(g-h)).

457 In the near-estuary reach, the ebb tidal flow consists of runoff discharge and the  
458 flood tidal current, both of which are relatively stable at the yearly time scale (Zhu et

459 al., 2017, 2018). Consequently, the yearly ebb tidal flow is also stable, implying that  
460 ebb partition ratios in the branching channels determine the allocation of ebb tidal  
461 amplitudes among these channels. Existing theory has established that the ebb tidal  
462 force dominates channel evolution in tide-affected reaches (Dou, 1964). Hence, the ebb  
463 partition ratio is responsible for morphological change in a branching channel. During  
464 a dry period with low runoff intensity (e.g. 2005-2007), the values of ebb partition ratio  
465 (i.e. ebb tidal force) for the south branch of Fujiangsha Waterway, the middle branch of  
466 Rugaosha Waterway, the east branch of Tongzhousha Waterway, and the east branch of  
467 Langshansha Waterway were large (Figs. 5(b, c, e, g)). Hence, downstream transport of  
468 sediment tended to occur in these channels, resulting in erosion or reduced deposition  
469 in the channels (Table 2); meanwhile, the channel depo-centers were pushed  
470 downstream by the strong ebb tidal current (Table 3). Conversely, the values of ebb  
471 partition ratio for other waterway branches were small (Figs. 5(a, d, f, h)), which  
472 promoted the relative strength of the flood tide in these channels, driving upstream  
473 sediment transport from downstream reaches into the channels, leading to deposition or  
474 reduced erosion (Table 2); simultaneously, the channel depo-centers were pushed  
475 upstream by the strong flood tidal current (Table 3). During flood periods of high runoff  
476 intensity (e.g. 2007-2011 and 2011-2014), the opposite occurred (Fig. 5; Table 2; Table  
477 3).

### 478 5.3 Trends in channel erosion-deposition and depo-center movement

479 The presence of dams caused decreases in duration days of discharges exceeding  
480 50,000 m<sup>3</sup>/s and 60,000 m<sup>3</sup>/s and increases in duration days of discharges in the range

481 10,000—20,000 m<sup>3</sup>/s (Fig. 3). This resulted in decreasing trends in ebb partition ratios  
482 for the north region of Fujiangsha Waterway, the Liuhaisha branch of Rugaosha  
483 Waterway, the west branch of Tongzhousha Waterway, and the west branch of  
484 Langshansha Waterway, and increasing trends for the other waterway branches (Fig. 4).  
485 Accordingly, a branching channel with decreasing ebb partition ratio presented a  
486 declining trend, and vice versa (Fig. 6; Chen et al., 2016). Meanwhile, depo-centers in  
487 declining branches tended to migrate upstream and become located in the upper sub-  
488 reaches, whereas those in developing branches tended to move downstream into the  
489 lower sub-reaches, as demonstrated for recent channel-regulation projects (Wu et al.,  
490 2013; Yang and Lin, 2013; Ni et al., 2014).

491 At the time of writing, a cascade of large dams is being constructed along the upper  
492 Yangtze, which will continue to flatten the intra-annual distribution of runoff discharge  
493 (Duan et al., 2016). In addition, the future change in climate will help promote this kind  
494 of runoff flattening (Cao et al., 2011; Sun et al., 2013; Zeng et al., 2013; Chai et al.,  
495 2019). Consequently, recent trends in ebb partition ratios, patterns of channel erosion-  
496 deposition, and depo-center movements in the near-estuary reach of the Yangtze are  
497 likely to persist well into the future.

## 498 **6 Conclusions**

499 The north region of Fujiangsha Waterway, the Liuhaisha branch of Rugaosha  
500 Waterway, the west branch of Tongzhousha Waterway, and the west branch of  
501 Langshansha Waterway in the near-estuary reach of the Yangtze River tend to  
502 experience increased deposition or reduced erosion in periods of low runoff intensity,



503 and vice versa. The depo-centers in these channels have been found to move upstream  
504 and downstream under low and high runoff intensity scenarios. Meanwhile, the other  
505 waterway branches in the near-estuary reach experience opposite trends in erosion-  
506 deposition pattern and depo-center movement with varying runoff intensity.

507 The mechanism behind the foregoing morphological changes relates to variations  
508 in ebb partition ratio in the branching channels as the flow hydrodynamics alters, owing  
509 partly to geographic features (raised nodes and connections among the branches) of the  
510 near-estuary reach. As runoff discharge rose, the ebb partition ratios in the north region  
511 of Fujiangsha Waterway, the Liuhaisha branch of Rugaosha Waterway, the west branch  
512 of Tongzhousha Waterway, and the west branch of Langshansha Waterway increased.  
513 Thus, sediment in these branching channels tended to be transported into downstream  
514 reaches by the ebb tidal current, resulting in erosion or reduced deposition, with the  
515 depo-centers pushed downstream. Ebb partition ratios in the other waterway branches  
516 decreased, with sediment in downstream reaches transported into the branches by the  
517 relatively stronger flood tidal current, leading to deposition or less erosion in the  
518 branches, and causing the depo-centers to migrate upstream. As runoff discharge fell,  
519 the opposite occurred.

520 The runoff-flattening effect of dams in Yangtze Basin has greatly decreased the  
521 duration days of flood discharges exceeding 50,000 m<sup>3</sup>/s and 60,000 m<sup>3</sup>/s, and increased  
522 those of the middle-low discharge between 10,000 and 20,000 m<sup>3</sup>/s. This in turn  
523 significantly reduced the values of ebb partition ratio in the north region of Fujiangsha  
524 Waterway, the Liuhaisha branch of Rugaosha Waterway, the west branch of

525 Tongzhousha Waterway, and the west branch of Langshansha Waterway. Therefore,  
526 these branching channels have presented declining morphological trends, with their  
527 depo-centers tending to move upstream, becoming located in the upper sub-reaches.  
528 Dam-induced runoff flattening has enhanced ebb partition ratios in the other waterway  
529 branches, promoting morphological development and downstream migration of depo-  
530 centers into the lower sub-reaches of the branches. As a cascade of large dams continues  
531 to be constructed along the upper Yangtze and climate change is ongoing, current  
532 overall trends in the evolution of branching channels and migration of depo-centers are  
533 likely to be maintained into the future.

534 Although the current study has mainly focused on a local tide-affected braided  
535 reach of the Yangtze River, it may be instructive for other braided rivers experiencing  
536 similar hydrodynamic processes, because of its representativeness in investigating the  
537 morphological evolution in intermediate zones between the fluvial and the estuarine  
538 areas. A numerical model, which gives a full consideration of water, sediment and  
539 engineering projects, will be set up in the next step to quantify the morphological  
540 evolution of this reach.

541 **Acknowledgements** This research was supported by open funding of the Key Laboratory of Water-  
542 Sediment Sciences and Water Disaster Prevention of Hunan Province (No. 2019SS06), and the  
543 National Key Research and Development Program of China (No. 2018YFC0407201 and No.  
544 2016YFC0402306).

## 545 **Reference**

546 Alcayaga H, Palma S, Caamano D, Mao L, Soto-Alvarez M (2019). Detecting and quantifying

547 hydromorphology changes in a Chilean river after 50 years of dam operation. *Journal of South*  
548 *American Earth Sciences*, 93: 253-266

549 Cao L J, Zhang Y, Shi Y (2011). Climate change effect on hydrological processes over the Yangtze  
550 River basin. *Quaternary International*, 244(2): 202-210

551 Chai Y F, Li Y T, Yang Y P, Zhu B Y, Li S X, Xu C, Liu C C (2019). Influence of climate variability  
552 and reservoir operation on streamflow in the Yangtze River. *Scientific Reports*, 9: 5060

553 Changjiang Water Resources Commission (CWRC) (2016). *Changjiang River Sediment Bulletin*.  
554 Wuhan: Changjiang Press (in Chinese)

555 Chen J Y, Shen H T, Yun C X, eds (1988). *Processes of Dynamics and Geomorphology of the*  
556 *Changjiang Estuary*. Shanghai: Shanghai Scientific & Technical Publishers (in Chinese)

557 Chen Y P, Jiang N L, Zhang C K (2012). Riverbed evolution of upper part of Yangtze Estuary and  
558 its response to the hydrodynamic changes at upstream. In: *Proceedings of the 33<sup>rd</sup> International*  
559 *Conference on Coastal Engineering*. Reston: ASCE Press, 1-6

560 Chen Y P, Li J X, Wu Z G, Pan S Q (2016). Dynamic analysis of riverbed evolution: Chengtong  
561 Reach of Yangtze Estuary. *Journal of Coastal Research*, 75: 203-207

562 Dai W H, Ding W (2019). Hydrodynamic improvement of a goose-head pattern braided reach in  
563 lower Yangtze River. *Journal of Hydrodynamics*, 31(3): 614-621

564 Dou G R (1964). The bed form of the alluvial streams and the tidal delta. *SHUILI XUEBAO*, 1964:  
565 1-13 (in Chinese)

566 Duan W X, Guo S L, Wang J, Liu D D (2016). Impact of cascaded reservoirs group on flow regime  
567 in the middle and lower reaches of the Yangtze River. *Water*, 8(6): 218

568 Fan Y Y, Li Y T, Yang Y P, Huang L B (2017). Vertical velocity structure distribution in the Sansha

569 area of the Yangtze Estuary, China. *Journal of Marine Science and Technology*, 22(2): 327-334

570 Graf W L (2006). Downstream hydrologic and geomorphic effects of large dams on American rivers.

571 *Geomorphology*, 79(3-4): 336-360

572 Han J Q, Zhang W, Yuan J, Fan Y Y (2018). Channel evolution under changing hydrological regimes

573 in anabranching reaches downstream of the Three Gorges Dam. *Frontiers of Earth Science*,

574 12(3): 640-648

575 Horrevoets A C, Savenije H H G, Schuurman J N, Graas S (2004). The influence of river discharge

576 on tidal damping in alluvial estuaries. *Journal of Hydrology*, 294(4): 213-228

577 Jain V, Sinha R (2004). Fluvial dynamics of an anabranching river system in Himalayan foreland

578 basin, Bagmati river, north Bihar plains, India. *Geomorphology*, 60(1-2): 147-170

579 Jansen J D, Nanson G C (2010). Functional relationships between vegetation, channel morphology,

580 and flow efficiency in an alluvial (anabranching) river. *Journal of Geophysical Research – Earth*

581 *Surface*, 115: F04030

582 Jiang C J, Li J F, de Swart H E (2012a). Effects of navigational works on morphological changes in

583 the bar area of the Yangtze Estuary. *Geomorphology*, 139: 205-219

584 Jiang N L, Chen Y P, Zhang C K (2012b). Channel evolution of Chengtong reach at Yangtze Estuary.

585 In: *Proceedings of the 22<sup>nd</sup> (2012) International Offshore and Polar Engineering Conference*.

586 San Francisco: ISOPE Press, 1382-1386

587 Kaliraj S, Chandrasekar N, Magesh N S (2014). Impacts of wave energy and littoral currents on

588 shoreline erosion/accretion along the south-west coast of Kanyakumari, Tamil Nadu using

589 DSAS and geospatial technology. *Environmental Earth Sciences*, 71(10): 4523-4542

590 Kuang C P, Chen W, Gu J, He L L (2014). Comprehensive analysis on the sediment siltation in the

591 upper reach of the deepwater navigation channel in the Yangtze Estuary. *Journal of*  
592 *Hydrodynamics*, 26(2): 299-308

593 Latrubesse E M (2008). Patterns of anabranching channels: The ultimate end-member adjustment  
594 of mega rivers. *Geomorphology*, 101(1-2): 130-145

595 Li M T, Chen Z Y, Yin D W, Chen J, Wang Z H, Sun Q L (2011). Morphodynamic characteristics of  
596 the dextral diversion of the Yangtze River mouth, China: tidal and the Coriolis Force controls.  
597 *Earth Surface Processes and Landforms*, 36(5): 641-650

598 Li M T, Ge J Z, Kappenberg J, Much D, Nino O, Chen Z Y (2014). Morphodynamic processes of  
599 the Elbe River estuary, Germany: the Coriolis effect, tidal asymmetry and human dredging.  
600 *Frontiers of Earth Science*, 8(2): 181-189

601 Li Z W, Yu G A, Brierley G, Wang Z Y (2016). Vegetative impacts upon bedload transport capacity  
602 and channel stability for differing alluvial planforms in the Yellow River source zone. *Hydrology*  
603 *and Earth System Sciences*, 20(7): 3013-3025

604 Liu F, Hu S, Guo X J, Luo X X, Cai H Y, Yang Q S (2018). Recent changes in the sediment regime  
605 of the Pearl River (South China): Causes and implications for the Pearl River Delta.  
606 *Hydrological Processes*, 32(12): 1771-1785

607 Luan H L, Ding P X, Wang Z B, Ge J Z, Yang S L (2016). Decadal morphological evolution of the  
608 Yangtze Estuary in response to river input changes and estuarine engineering projects.  
609 *Geomorphology*, 265: 12-23

610 Mendoza A, Soto-Cortes G, Priego-Hernandez G, Rivera-Trejo F (2019). Historical description of  
611 the morphology and hydraulic behavior of a bifurcation in the lowlands of the Grijalva River  
612 Basin, Mexico. *Catena*, 176: 343-351

613 Ni B, He R, Zhang W (2014). Study on dredging scale of Tongzhousha west channel. *Journal of*  
614 *Waterway and Harbor*, 35(6): 608-612 (in Chinese)

615 Petts G E, Gurnell A M (2005). Dams and geomorphology: Research progress and future directions.  
616 *Geomorphology*, 71(1-2): 27-47

617 Rangoonwala A, Jones C E, Ramsey E (2016). Wetland shoreline recession in the Mississippi River  
618 Delta from petroleum oiling and cyclonic storms. *Geophysical Research Letters*, 43(22): 11652-  
619 11660

620 Schletterer M, Shaporenko S I, Kuzovlev V V, Minin A E, Van Geest G J, Middelkoop H, Gorski K  
621 (2019). The Volga: Management issues in the largest river basin in Europe. *River Research and*  
622 *Applications*, 35(5): 510-519

623 Shen Y M, Deng G F, Xu Z H, Tang J (2019). Effects of sea level rise on storm surge and waves  
624 within the Yangtze River Estuary. *Frontiers of Earth Science*, 13(2): 303-316

625 Sloff K, Van Spijk A, Stouthamer E, Sieben A (2013). Understanding and managing the morphology  
626 of branches incising into sand-clay deposits in the Dutch Rhine Delta. *International Journal of*  
627 *Sediment Research*, 28(2): 127-138

628 Sun J L, Lei X H, Tian Y, Liao W H, Wang Y H (2013). Hydrological impacts of climate change in  
629 the upper reaches of the Yangtze River Basin. *Quaternary International*, 304: 62-74

630 Wang Y H, Dong P, Oguchi T, Chen S L, Shen H T (2013). Long-term (1842-2006) morphological  
631 change and equilibrium state of the Changjiang (Yangtze) Estuary, China. *Continental Shelf*  
632 *Research*, 56: 71-81

633 Warne A G, Guevara E H, Aslan A (2002). Late Quaternary evolution of the Orinoco Delta,  
634 Venezuela. *Journal of Coastal Research*, 18(2): 225-253

635 Wu Z G, Chen Y P, Zhang C K, Jiang N L (2013). Fluvial dynamic analysis of Rugaosha reach in  
636 Changjiang Estuary. *Yangtze River*, 44(24): 13-16+19 (in Chinese)

637 Xu Y, Gong H F, Zhang H (2014). Study on branch selection for 12.5 m - deep main channel in  
638 Fujiangsha reach downstream the Changjiang River. *Port & Waterway Engineering*, 2014(5): 1-  
639 7 (in Chinese)

640 Yang S L, Milliman J D, Li P, Xu K (2011). 50,000 dams later: Erosion of the Yangtze River and its  
641 delta. *Global and Planetary Change*, 75(1-2): 14-20

642 Yang S L, Xu K H, Milliman J D, Yang H F, Wu C S (2015). Decline of Yangtze River water and  
643 sediment discharge: Impact from natural and anthropogenic changes. *Scientific Reports*, 5:  
644 12581

645 Yang X W, Lin Q (2013). Evolution analysis and maintenance countermeasures of north channel of  
646 Fujiang shoal in Lower Yangtze River. *Journal of Waterway and Harbor*, 34(1): 50-54 (in  
647 Chinese)

648 Yu W C, eds (2013). *Understanding and Practice of the Yangtze River*. Beijing: China Water &  
649 Power Press (in Chinese)

650 Yun C X, eds (2004). *Recent Developments of the Changjiang Estuary*. Beijing: China Ocean Press  
651 (in Chinese)

652 Zeng X F, Zhao N, Zhou J Z (2013). Study on hydropower energy and its future changes in the  
653 upper Yangtze River basin under climate change. *Advanced Research on Material, Energy and  
654 Control Engineering*, 648: 232-236

655 Zhang W, Xu P (2017). Morphological relationships of runoff tidal estuary on the lower reaches of  
656 the Yangtze River. *China Harbour Engineering*, 37(1): 19-23 (in Chinese)

- 657 Zhang W, Xu Y, Hoitink A J F, Sassi M G, Zheng J H, Chen X W, Zhang C (2015). Morphological  
658 change in the Pearl River Delta, China. *Marine Geology*, 363: 202-219
- 659 Zhao J, Guo L C, He Q, Wang Z B, van Maren D S, Wang X Y (2018). An analysis on half century  
660 morphological changes in the Changjiang Estuary: Spatial variability under natural processes  
661 and human intervention. *Journal of Marine Systems*, 181: 25-36
- 662 Zheng S W, Cheng H Q, Shi S Y, Xu W, Zhou Q P, Jiang Y H, Zhou F N, Cao M X (2018). Impact  
663 of anthropogenic drivers on subaqueous topographical change in the Datong to Xuliujing reach  
664 of the Yangtze River. *Science China - Earth Sciences*, 61(7): 940-950
- 665 Zhou Y Y, Huang H Q, Ran L S, Shi C X, Su T (2018). Hydrological controls on the evolution of  
666 the Yellow River Delta: An evaluation of the relationship since the Xiaolangdi Reservoir became  
667 fully operational. *Hydrological Processes*, 32(24): 3633-3649
- 668 Zhu B Y, Deng J Y, Yue Y, Li Z W, Zhang C C (2019). Responses of erosion and deposition in  
669 braided reaches between Datong and Jiangyin to varying water and sediment discharges in lower  
670 Yangtze River. *Taiwan Water Conservancy*, 67(2): 46-57 (in Chinese)
- 671 Zhu B Y, Li Y T, Yang P Y, Deng J Y, Yang Y P, Li S X (2018). River bed erosion and deposition  
672 responses to sediment reduction in the Chengtong reach of the Yangtze River. *Advances in Water  
673 Science*, 29(5): 706-716 (in Chinese)
- 674 Zhu B Y, Li Y T, Yue Y, Yang Y P (2017). Aggravation of north channels' shrinkage and south  
675 channels' development in the Yangtze Estuary under dam-induced runoff discharge flattening.  
676 *Estuarine Coastal and Shelf Science*, 187: 178-192

## 677 **Author biographies**

- 678 **□** Boyuan ZHU



679 Water Conservancy and Hydropower Engineering, B.S., Wuhan University, Wuhan,  
680 China, 2011

681 Hydraulics and River Dynamics, Ph.D, Wuhan University, Wuhan, China, 2017

682 Dr. Zhu served as a technical professional in Zhongnan Engineering Corporation  
683 Limited of Power China during 2017-2018, before taking up a teaching position at  
684 Changsha University of Science & Technology from 2018. His research interests  
685 include sediment transport and river evolution.

686 The email address of Dr. Zhu is: [boyuan@csust.edu.cn](mailto:boyuan@csust.edu.cn)

687 **□ Jinyun DENG**

688 Port, Channel and River Regulation, B.S., Wuhan University, Wuhan, China, 1998

689 Hydraulics and River Dynamics, M.S., Wuhan University, Wuhan, China, 2000

690 Hydraulics and River Dynamics, Ph.D, Wuhan University, Wuhan, China, 2003

691 Prof. Deng gained a teaching position in Wuhan University in 2003 and was  
692 appointed associate professor in 2006. His research interests include sediment  
693 transport and river evolution.

694 The email address of Prof. Deng is: [dengjinyun@whu.edu.cn](mailto:dengjinyun@whu.edu.cn)

695 **□ Jinwu TANG**

696 Port, Channel and River regulation, B.S., Wuhan University, Wuhan, China, 2007

697 Hydraulics and River Dynamics, Ph.D, Wuhan University, Wuhan, China, 2012

698 Dr. Tang is a technical professional in Changjiang Institute of Survey, Planning,  
699 Design and Research, where he has been employed since 2012. His research  
700 interests include river planning and management.

701 The email address of Dr. Tang is: [tangjinwu1106@163.com](mailto:tangjinwu1106@163.com)

702 **□ Wenjun YU**

703 Water Conservancy and Hydropower Engineering, B.S., Xi'an University of  
704 Technology, Xi'an, China, 2012

705 Hydraulics and River Dynamics, M.S., Wuhan University, Wuhan, China, 2015

706 Mr. Yu is a technical professional in Changjiang Waterway Institute of Planning,  
707 Design & Research, where he has been employed since 2015. His research interests  
708 include river regulation and management.

709 The email address of Mr. Yu is: [y430011@sina.cn](mailto:y430011@sina.cn)

710 **□ Alistair G.L. BORTHWICK**

711 Civil engineering, BEng (1st class), University of Liverpool, Liverpool, UK, 1978

712 PhD, University of Liverpool, Liverpool, UK, 1982

713 MA, University of Oxford, Oxford, UK, 1990

714 DSc, University of Oxford, Oxford, UK, 2007

715 Prof. Borthwick was previously professor of engineering science at the University  
716 of Oxford, where he worked for 21 years from 1990-2011. He is presently a  
717 professorial fellow at the University of Edinburgh. His research interests include  
718 coastal and offshore engineering, environmental fluid mechanics, and marine  
719 power resource assessment.

720 Prof. Borthwick has 40 years' engineering, research, and teaching experience. He  
721 was elected a Fellow of the Institution of Civil Engineers, FICE, in 2003, a Fellow  
722 of the Royal Academy of Engineering, FREng, in 2014, and a Fellow of the Royal

723 Society of Edinburgh, FRSE, in 2015.

724 His email address is: [Alistair.Borthwick@ed.ac.uk](mailto:Alistair.Borthwick@ed.ac.uk)

725  Yuanfang CHAI

726 Agricultural Water Conservancy Engineering, B.S., Taiyuan University of

727 Technology, Taiyuan, China, 2016

728 Hydraulics and River Dynamics, M.S., Wuhan University, Wuhan, China, 2019

729 Mr. Chai's research interests include sediment transport and river evolution.

730 His email address is: [2808676930@qq.com](mailto:2808676930@qq.com)

731  Zhaohua SUN

732 Port, Channel and River Regulation, B.S., Wuhan University, Wuhan, China, 1999

733 Hydraulics and River Dynamics, Ph.D, Wuhan University, Wuhan, China, 2004

734 Prof. Sun took up a teaching position in Wuhan University in 2004 and has since

735 been appointed associate professor. His research interests include sediment

736 transport and river evolution.

737 His email address is: [Lnszh@126.com](mailto:Lnszh@126.com)

738  Yitian LI

739 Port, Channel and River Regulation, B.S., Wuhan University, Wuhan, China, 1981

740 Hydraulics and River Dynamics, Ph.D, Wuhan University, Wuhan, China, 1987

741 Prof. Li has been employed by Wuhan University for 32 years, where he is senior

742 professor in river engineering. His research interests include sediment transport and

743 river evolution.

744 Prof. Li is vice director of the Sediment Committee of the Chinese Hydraulic

745        Engineering Society. He has won two Second Class Prizes for the Scientific and

746        Technological Progress of China. His email address is: [ytli@whu.edu.cn](mailto:ytli@whu.edu.cn)

747